Military Technical College
Kobry El-Kobbah,
Cairo, Egypt.

16th International Conference
on Applied Mechanics and
Mechanical Engineering.

A COMPUTATIONAL STUDY OF IN-CYLINDER FLOW CHARACTERISTICS IN TWO STROKE SIE WITH DOUBLE INTAKE MANIFOLDS AT DIFFERENT INCLINATION ANGLES

M. S. Radwan*** , O. S. M. Abu El-Yazeed**, I. Elbadawy** and M. M. Gad*

ABSTRACT

This investigation is carried out to simulate the in-cylinder non-reacting flow of a two stroke spark ignition internal combustion engine (SIE) with gasoline direct injection (GDI). Computer Aided Design (CAD) model was built based on the LUPOE-2D two stroke SIE geometries that had been used in experimental previous work. The computational fluid dynamics (CFD) analysis technique is used to predict in-cylinder flow turbulence levels, including root-mean square (RMS) turbulent velocity. The three dimensional domain is created using FLUENT-ANSYS 14.0. The mathematical model is validated against previous experimental data. The intake manifold inclination angles of 0, 10, 20, 30 and 40° are investigated of double intake manifold at engine speed of 1500 rpm. The results indicate that the highest RMS turbulent velocities are achieved at 30° inclination angle of the inlet manifold at the crank angles of 24, 17, 10° before top dead center BTDC and 0° at top dead center TDC. Also, it is found that, the maximum RMSs occur at 0.18 of the radius of the cylinder at crank angle of 24° BTDC but at 0.25 of the radius at crank angles of 17, 10° BTDC and 0° at TDC.

KEYWORDS

Two stroke engine, Numerical simulation, Turbulence

---

* PG student, Dept. of Mechanical Power Engineering, Faculty of Engineering at El-Mattaria, Helwan University, P.O., Cairo 11718, Egypt.

** Assistant Professor, Dept. of Mechanical Power Eng., Faculty of Engineering at El-Mattaria, Helwan University, P.O., Cairo 11718, Egypt.

*** Professor, Dept. of Mechanical Power Eng., Faculty of Eng. at El-Mattaria, Helwan University, Cairo 11718, Egypt

INTRODUCTION

Two-stroke spark ignition engines (SIEs) are suffering from high emissions and poor fuel economy compared to four stroke engines [1]. The major pollutants of the two-stroke (SIEs) are carbon monoxide and unburned hydrocarbons (UBHC). Therefore, globally, strict regulations are made for permissible levels of pollutants in the exhaust of two-stroke SIEs.

While, the basic goals of the automotive industry are high power, low specific fuel consumption, low emissions, low noise and better comfortable drive. Recently, the automotive industry is interested in the two-stroke engine due to its lower weight, volume compact body and theoretical twice in power compared to four-stroke engines of same cubic capacity [2]. Two stroke SIEs are employed in light transportation applications such as motorcycles, small yachts, chainsaws, outboard motors, etc.

Carburetion was the first system used to mix fuel and air [3].This was later improved by the advent of port fuel injection (PFI). Heywood [4] describes that in PFI systems the fuel is injected into the intake port/manifold of each cylinder. In PFI, there is a time lag between the injection event and the induction of the fuel and air mixture into the cylinder [5].

The gasoline direct injection (GDI) engines, in which the fuel is injected directly into the cylinder, are a common alternative to port fuel injection (PFI) engines. In PFI engines, large droplet diameters of the order of 120 μm at low injection pressures, namely 2.5-4.5 bar can result [5]. However, these are usually not a serious problem because there is enough time to mix and evaporate fuel in the intake manifold before entering the cylinder. The injection pressure plays a much more important role in GDI engines because fuel is injected directly into the cylinder and must be evaporated very rapidly. As a result, high injection pressures, namely 40-130 bar [5] are generally used in GDI engines to improve both atomization and evaporation. GDI engines have significant advantages over the PFI engines such as improving fuel consumption, hence reducing CO_2 emissions, quick start, improved transient response and precise Fuel/Air ratio control.

Gasoline direct injection (GDI) two-stroke engines reduce the UBHC by 88% and Carbon monoxide by 72% compared with a carbureted system [6]. In addition to the fuel consumption improved by 32% due to the near elimination of short circuiting losses as well as more complete combustion [7].

Krishna and Mallikarjuna [7] concluded that increasing turbulence intensity is believed to generate higher flame speed and high reactive flame surface area. The turbulence controls the rate of flow dissipation, heat transfer and the rate of flame propagation and it is quantified by turbulent kinetic energy (TKE) within the cylinder [8]. Moreover, the turbulent flow has a high influence on flame propagation and deviations of the flame kernel from spherical as the air to fuel ratio is increased, with much higher probability of influence of velocity fluctuations [9 and 10]. Consequently, turbulent flow has high influence on the internal combustion engine because as it effects in increasing efficiency, reducing of knock and improving combustion instability [11].

In-cylinder flow structure has a significant influence on the internal combustion engine as on mixing of air- fuel, combustion process and burning rate. The GDI engine development is mainly concerned in the study of air fuel interaction; as for injecting fuel directly in to the cylinder. The analysis of in-cylinder flow and air-fuel interaction is important for air-fuel mixing and fuel vaporization. Intake flow pattern depends on moving piston also creates large scale rotating flow pattern within the cylinder [12]. High turbulence intensity is one of the most important factors for stabilizing the ignition process and fast propagation of flame, especially in case of lean-burn combustion. Two types of vortices are utilized in order to generate and preserve the turbulent flow efficiently. They are known as swirl and tumble flows, which are organized rotations in the horizontal and vertical plane of the engine cylinder, respectively. Both are created during the intake stroke [8 and 13].

Kang and Baek [14] reported that the turbulence intensity with tumble flow at the end of compression is twice of that without tumble. Moreover, tumble flow can be used in homogeneous and stratified combustion, depending on the injector location and fuel flow direction relative to the tumble motion [15 and 16]. The intake port inclination has high influence on the in-cylinder flow motion, where upright straight intake ports are used to produce a strong tumble which can enhance turbulence levels and shows promise for generation of strong tumble [17 and 18].

In GDI engines, swirl is used to enhance the air–fuel mixing for emission control and better volumetric efficiency [5]. The brake specific fuel consumption is decreased with increasing turbulence intensity steadily [19 and 20].

Internal combustion engine performance and exhaust emissions are governed by unsteady fluid dynamic process. Computational Fluid Dynamic (CFD) analysis is a solution of fluid motion equation usually partial differential equations (PDE) type using numerical approximation. This process is called discretization turns the PDEs into simultaneous algebraic equations. Such equations are solved using algebraic solution techniques, usually iterative method [21].

The approximations are applied to a number of small domains in space and times called grid. Therefore, the final results are spatially and temporally resolved. Using CFD, enables building a computational model represented the direct injection two stroke SIE to be studied. Then, the fluid flow equations can be applied to the prototype and the fluid dynamics will be predicted by the software. As a result, CFD is a highly developed computationally based design and analysis technique [2].

MATHEMATICAL MODEL

Governing Flow Equations

The in-cylinder air flow was modeled by the Navier-Stokes and continuity equations, namely:

$$\frac{\partial}{\partial t}(\rho\bar{u}) + \nabla.(\rho\bar{u}\bar{u}) = -\nabla p + \nabla.\bar{\bar{\tau}} + \rho\bar{g} \quad (1)$$

$$\frac{\partial \rho}{\partial t} + \nabla.(\rho\bar{u}) = 0 \quad (2)$$

where ρ is the density of the gas, p is the pressure, $\bar{u}(=u\bar{\imath}+v\bar{\jmath}+w\bar{k})$ is the gas velocity vector, g is the acceleration due to gravity and

$$\bar{\bar{\tau}} = \mu\left[\nabla.\bar{u} + (\nabla.\bar{u})^T - \frac{2}{3}\nabla.\bar{u}.\bar{\bar{I}}\right] \quad (3)$$

is the Newtonian stress tensor, where $\bar{\bar{I}}$ is the unit tensor.

Practically, turbulence played an important role in enhancing fuel mixing, evaporation and increase of burning velocity. Therefore, in the present study the effects of turbulence are modeled using Reynolds Average Navier-Stokes (RANS) approaches that have been performed successfully in previous related work. These included the *k-ε* model [22], is recommended by previous mentioned researchers [19]. The *k-ε* turbulence model based on two extra transport equations for turbulent kinetic energy, k, and the turbulent dissipation rate ε, which are given by

$$\frac{\partial(\rho k)}{\partial t} + \frac{\partial(\rho k\bar{u}_j)}{\partial x_j} = \frac{\partial}{\partial x_j}\left[\left(\mu + \frac{\mu_t}{\sigma_k}\right)\frac{\partial k}{\partial x_j}\right] + G_k - \rho\varepsilon \quad (4)$$

$$\frac{\partial(\rho\varepsilon)}{\partial t} + \frac{\partial(\rho\varepsilon\bar{u}_j)}{\partial x_j} = \frac{\partial}{\partial x_j}\left[\left(\mu + \frac{\mu_t}{\sigma_\varepsilon}\right)\frac{\partial \varepsilon}{\partial x_j}\right] + C_{\varepsilon 1}\frac{\varepsilon}{k}G_k - C_{\varepsilon 2}\rho\frac{\varepsilon^2}{k} \quad (5)$$

respectively. Where, $C_{\varepsilon 1}$, $C_{\varepsilon 2}$and C_μ are adjustable constants. σ_k and σ_ε are Prandtl numbers for k and ε, respectively.

Computational Model

Computer Aided Design (CAD) model was built based on the LUPOE-2D two stroke SIE geometries, shown in Fig. 1, that had been used by Burluka et al. [23]. The flat piston of this engine was suitable for combustion chamber of direct injection SI engine compared to other piston configurations in terms better TKE, high tumble ratio (TR), ignitable air-fuel mixture at the spark plug location, better power output and easy of piston manufacturing [12]. The engine dimensions are indicated in Table 1.

Table 1: Engine Dimensions

Bore (mm) / Stroke (mm)	80 /112
Connecting-Rod Length (mm)	232
Clearance Height (mm)	8
Inlet Port Open/Close	107.8°(A/BTDC)
Exhaust Port Open/Close	101.4° (A/BTDC)

The cylinder geometry is generated by ANSYS 14.0 as indicated in Fig.2. The cylinder volume is divided into 63 separated volumes such as Inlet ports volumes, Exhaust ports volumes and cylinder volume. Figure 3 shows the mesh of volumes which is generated using T-GRID type of mesh to fulfill the requirement of the

dynamic mesh method [11]. Layered hexahedral mesh type is specified for moving part and unstructured tetrahedral elements for stationary region [21].

The dynamic mesh model in FLUENT is used to model flow as the shape of the domain is changing with time due to motion of the domain boundaries. In this case, dynamic mesh is set to calculate the piston location. Such location is proportional to the crank angle (θ). The update of the volume mesh is handled automatically by FLUENT at each time step based on the new location of the boundaries as mentioned by Semin et al. [24].

Boundary Conditions

The working fluid is air, the inlet ports are inclined with the horizontal by an inclination angle (α) of 40o and the inlet flow rate is 6.9 gm/sec/port according to the experimental data by Burluka et al. [23]. All the boundaries should be defined as pressure boundaries at which the pressure is atmospheric. The face between the volumes of the ports and cylinder is defined as sliding interface. Events are used to control the timing of opening and closure of the ports. The pressure velocity coupling should be set up to standard. The under relaxation factors are changed according to each case, in this case the momentum is set to be 0.5 and all other parameters are kept as default. There are three dynamics mesh methods applicable in FLUENT that are Smoothing, Layering and Remeshing. Under in-cylinder conditions, the parameters are set to follow the experimental operating conditions as presented in Table 2.

Table 2: Operating conditions

Parameters	Value
Crank Shaft Speed (rpm)	1500
Starting Crank Angle (deg)	180
Crank Period (deg)	360
Crank Angle Step Size (deg)	1
Piston Stroke (m)	0.112
Connecting Rod Length (m)	0.232
Piston Stroke Cutoff (m)	0.008
Intake mass flow rate (gm/s)	6.9
Inlet air Pressure (atm)	1
Inlet air Temperature (k)	300

RESULTS AND DISCUSSION

Before carrying out the whole simulation work with FLUENT the results are validated against experimental results of Burluka et al. [23] at the same operating conditions mentioned in Table 2. The mesh independent study is performed at 3, 4 and 5 mm mesh sizes. The RMS turbulent velocity (u') is the key parameter of validation. It is calculated over a range of crank angles (θ) of 45° before top dead center (BTDC) to 45° after to dead center (ATDC) at a center point of the mid plan of the clearance volume. As shown in Fig. 4, the results show that 3 mm and 4 mm mesh sizes yield a better agreement with each other and the experimental results than the 5 mm

mesh size. Therefore, all subsequent results are obtained using 4 mm mesh size to save the computing time. Using the selected mesh size of 4 mm, additional comparisons between experimental and computational results of u' along y-axis at θ= 0°, 10°, 17° and 24° BTDC are obtained as revealed in Fig. 5. According to Figs. 4 and 5, a good agreement is achieved.

According to [11, 12, and 25] the fuel is injected into the cylinder within a crank angle period from θ = 30° to 20° BTDC. Advanced injection timing caused piston wetting and retarded injection timing decreases sufficient time for fuel to air mixing. Therefore, θ= 24° BTDC was chosen in order to study the turbulence levels at fuel injection process. Also, the ignition timing is from 20° to 10° BTDC as reported in [7, 9 and 10]. For this reason, θ= 17° BTDC is selected to monitor the turbulence levels during the ignition time.

Due to a significant influence of the turbulence levels on the flame speed and propagation, θ= 10° BTDC and θ= 0° at TDC are selected in the present study in order to identify the turbulence levels during the flame propagation [7, 8, 10 and 20]. As shown in Figs. (6) to (9), the results are implemented by comprising the variation of u' with the cylinder radius, in terms of radius ratio, , γ $(=\frac{r}{R})$,where R is the cylinder radius. The parameter "r" is the radius along y-axis in the mid plan of clearance volume. These figures give u' at (θ = 10°, 17°, 24° BTDC and 0o at TDC) at different intake manifold angles (□ = 0o, 10°, 20°, 30° and 40°) for double intake port engine.

In-Cylinder Flow

The results show the effect of the inclination angle of the intake manifold of the double port engine on the turbulent velocity u' at different crank angles of (θ = 24°, 17°, 10° BTDC and 0° at TDC) as shown in Figs. 6, 7, 8 and 9, respectively. These results exhibit the same bell shape behavior whereas, the maximum turbulent velocities are located at γ = 0.18 at crank angle of 24° BTDC and γ = 0.25, at crank angles of (θ = 17°, 10° BTDC and 0o at TDC). By noticing that the results at the crank angles of (θ = 10° BTDC and 0o at TDC) exhibit very small difference between the velocities u' at inclination angles of (α = 30° and 20°). Thus, such maximum velocities u' of (3.9, 3.75, 3.4 and 3.02 m/s) are achieved at the crank angles of (θ = 24°, 17°, 10° BTDC and 0° at TDC), respectively, and at the inclination angle of the inlet manifold of (α = 30o). The maximum percentages of increasing of the turbulent velocities due to change of the inclination angles of the intake manifold are as the following (5.13, 5.33, 8.57 and 10%) at the crank angles of (θ = 24°, 17°, 10° BTDC and 0° at TDC), respectively.

As shown in Fig. 6 at crank angle of θ = 24° BTDC, the mixing of fuel and air is expected to be the highest at γ = 0.18 and α = 30°. Therefore, the injected fuel cone has to be directed to the position of γ = 0.18 to obtain the best fuel-air mixing process.

Figure 7 at crank angle of θ = 17° BTDC shows that the ignition energy needed for combustion of the mixture is expected to be increased for double inlet ports engine that if the spark plug is put at γ = 0.25 as stated by Haywood [4]. Thus, the position

of the spark plug has to be put at the center of the cylinder to minimize the needed ignition energy at low u' of 3.36 m/s.

At θ = 17° BTDC and θ = 0° TDC shown in Figs. 8 and 9, the results illustrate that the burning velocity and flame speed of the mixture is expected to be increased due to the increasing of turbulence intensity at inclination angle of the intake manifold of $\alpha = 30^o$ as well as at $\alpha = 20^o$.

According to the above discussion, the high values of u' and turbulence intensity are achieved at θ = 0°. As a result, u' contours are represented in Fig. 10 at $\alpha = 0^o$, 10°, 20°, 30° and 40°. Two separated vortices are formed due to double intake ports for all inclination angles. The maximum value of u' is achieved at $\alpha = 30^o$.

CONCLUSIONS

According to the study presented in this work, the following conclusions may be drawn:

1. The present model gives good agreement with the previous experimental data.
2. The inclination angle of the intake manifold of $\alpha = 30^o$ provide the highest turbulence levels of the double intake port engine compared with the other inclination angles of $\alpha = 0^o$, 10°, 20° and 40°.
3. The mixing of fuel and air is expected to be the highest at γ = 0.18 and $\alpha = 30^o$. Thus, the injected fuel cone has to be directed to the position of γ = 0.18 to obtain the best mixing conditions of fuel and air in the double port engine.
4. The position of the spark plug has to be put at the center of the cylinder to minimize the needed ignition energy at low u' of 3.36 m/s.
5. The burning velocity and flame speed of the mixture is expected to be increased due to the increasing of turbulence intensity at inclination angle of the intake manifold of $\alpha = 30^o$ as well as at $\alpha = 20^o$.

REFERENCES

[1] M. I. L. Galdo and C. G. R. Vidal, "Simulation of the Scavenging Process in Two-Stroke Engines", Journal of InTech, Paper No. 978-953-51-0219-9, 2012.

[2] S. R. Pitta and R. Kuderu, "A Computational Fluid Dynamics Analysis on Stratified Scavenging System of Medium Capacity Two-Stroke Internal Combustion Engines", Journal of THERMAL SCIENCE: Vol. 12, Paper No. 33-42, 2008.

[3] Roger and Mayhew, "Engineering Thermodynamics Work and Heat Transfer", Longman Scientific & Technical, 4th Edition, 1992.

[4] Heywood, John B. "Internal Combustion Engine Fundamentals", McGraw Hill Inc., 4th Edition, 1988.

[5] F. Zhao, M. C. Lai and D.L. Harrington, "Automotive Spark-Ignited Direct-Injection Gasoline Engines", Journal of Elsevier, Progress in Energy Combustion Science, Paper No. 437–562, 1999.

[6] N. Lorenz, T. Bauer and B. Willson, “Design of a Direct Injection Retrofit Kit for Small Two-Stroke Engines”, Journal of SAE, Paper No. 32-0095, 2005.

[7] B. M. Krishna and J.M. Mallikarjuna, “Effect of Engine Speed on In-Cylinder Tumble Flows in a Motored Internal Combustion Engine - An Experimental Investigation Using Particle Image Velocimetry”, *Journal of Applied Fluid Mechanics*, Paper No. 1735-3645, 2009.

[8] K. M. Pandey and B. Roy, “CFD Analysis of Intake Valve for Port Petrol Injection SI Engine”, Global Journal of Researches in Engineering, Mechanical and Mechanics Engineering, Volume 12 Issue 5 Version 1.0, Paper No. 2249-4596, 2012.

[9] A. Burluka, A.M.T.A. El-Dein Hussin, Z. Y. Ling and C.G.W. Sheppard, “Effects of large-scale turbulence on cyclic variability in spark-ignition engine”, Journal of Elsevier, Experimental Thermal and fluid Science 43, Paper No. 13-22, 2012.

[10] C. R. Kumar and G. Nagarajan, “Investigation of Flow During Intake Stroke of A Single Cylinder Internal Combustion Engine”, ARPN Journal of Engineering and Applied Sciences, VOL. 7, NO. 2, Paper No. 1819-6608, 2012.

[11] M. B. Çelik and B. Özdalyan, “Gasoline direct injection”, Journal of InTech., Paper No. 978-953-307-116-9, 2010.

[12] B. Harshavardhan and J. M. Mallikarjuna, “CFD Analysis of in-Cylinder Flow and Air-Fuel Interaction on Different Combustion Chamber Geometry in DISI Engine”, International Journal on Theoretical and Applied Research in Mechanical Engineering, Volume-2, Issue-3, Paper No. 2319 – 3182, 2013.

[13] Priscilla and Meena P, “A Comprehensive Study On In-Cylinder IC Engine Due To Swirl Flow”, International Journal of Engineering Research & Technology, Vol. 2 Issue 7, Paper No. 2278-0181, 2013.

[14] Kang, K. Y. and Baek, J.H., "Tumble Flow and Turbulence Characteristics in a Small Four-Valve Engine", SAE, Paper No. 960265, 1996

[15] T. Kim, S. Noh, C. Yu and I. Kang, “Optimization of Swirl and Tumble in KMC 2.4L Lean Burn Engine”, SAE, Paper No. 940307, 1994.

[16] Kume, T., Y. Lwamoto, K. Lida, M. Murakami, K. Akishino and H. Ando, “Combustion Control Technologies for Direct Injection SI Engine”, *SAE Paper No.* 960600, 1996.

[17] Z. Mahmood, A. Chen, M. Yianneskis and G. Ganti, “On The Structure of Steady Flow Through Dual Intake Engine Ports”, International Journalfor Numerical MethodsinFluids, VOL. 23, Paper No. 1085-1 109, 1996.

[18] N. Dinler and N. Yucel, “Numerical Simulation of Flow and Combustion in an Axisymmetric Internal Combustion Engine”, International Journal of Engineering and Applied Sciences, 2008.

[19] S.L. Yang, Y.K. Siow, C.Y. Teo, K. Hanjalic, “A KIVA code with Reynolds-stress model for engine flow Simulation”, Journal of Elsevier, Energy, Paper No. 427–445, 2005.

[20] G. Fru, D. Th´evenin and G. Janiga, “Impact of Turbulence Intensity and Equivalence Ratio on the Burning Rate of Premixed Methane–Air Flames”, journal of energies, Paper No. 1996-1073, 2011.

[21] N. M. I. N. Ibrahim, Semin, R. A. Bakar, A. R. Ismail and I. Ali, “In-Cylinder Mass Flow Rate and Gas Species Concentration Simulation of Spark Ignition Engine”, Journal of Engineering and Applied Sciences, Paper No. 1795-1806, 2007.

[22] Launder, B. E. and Spalding, D. B.,"The Numerical Computation of Turbulent Flows", Computer Methods in Applied Mechanics and Engineering, Volume 3, Paper No. 269-289, 1974

[23] A. A. Burluka, A.M.T.A. Hussin, Z. Y. Ling and C.G.W. Sheppard, “Effects of large-scale turbulence on cyclic variability in spark-ignition engine”, Journal of Elsevier, Experimental Thermal and fluid Science 43, Paper No. 13-22, 2012.

[24] Semin, N.M.I.N. Ibrahim, R. A. Bakar and A. R. Ismail, “In-Cylinder Flow through Piston-Port Engines Modeling using Dynamic Mesh”, Journal of Applied Sciences Research, Paper No. 4(1): 58-64, 2008.

[25] W. Mitianiec and M. Forma, “Mixture Formation at Spray Guided Direct Injection in SI Two-Stroke Engine”, Journal of Bibiolteka Cyfrowa Politechniki Krakowskiej, Paper No.1897-6328, 2008.

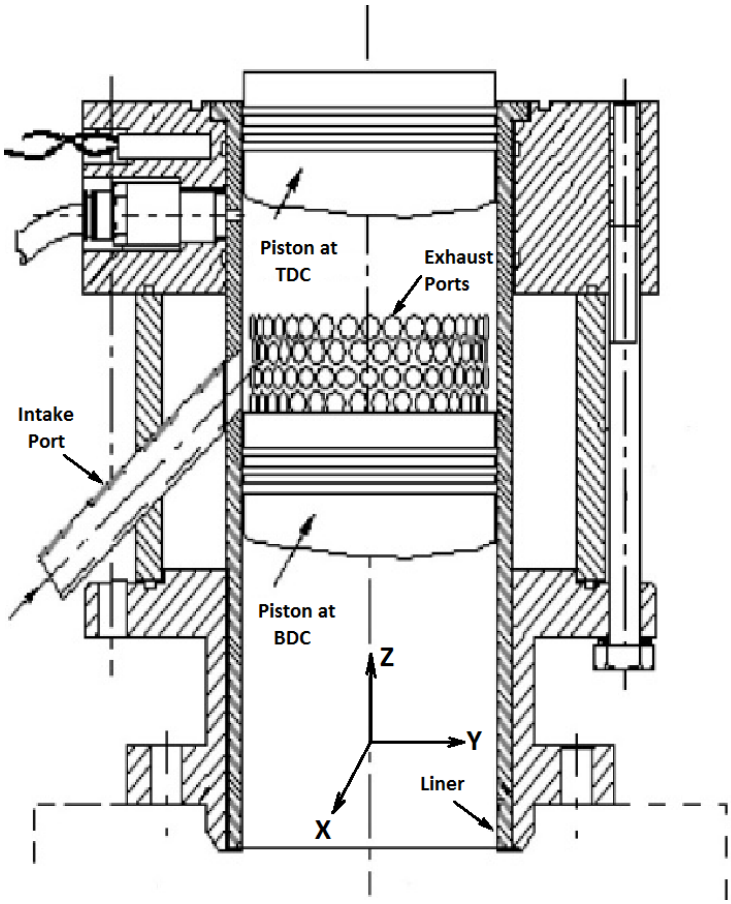

Fig. 1. Schematic of the LUPOE-2 engine; piston, liner, intake and exhaust ports [23].

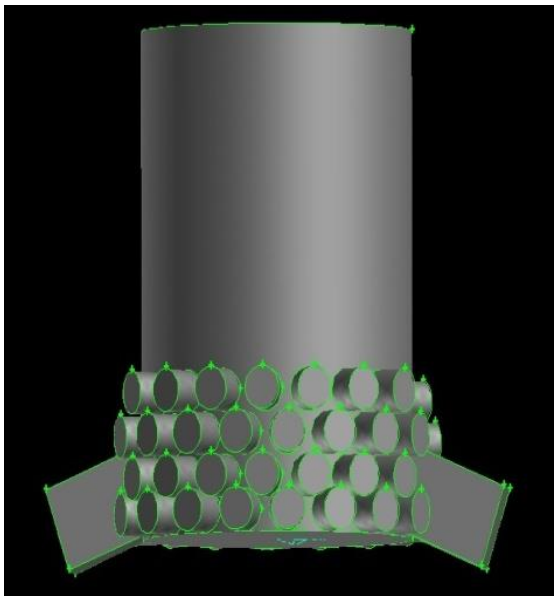

Fig. 2. 3D cylinder geometry generated by ANSYS.

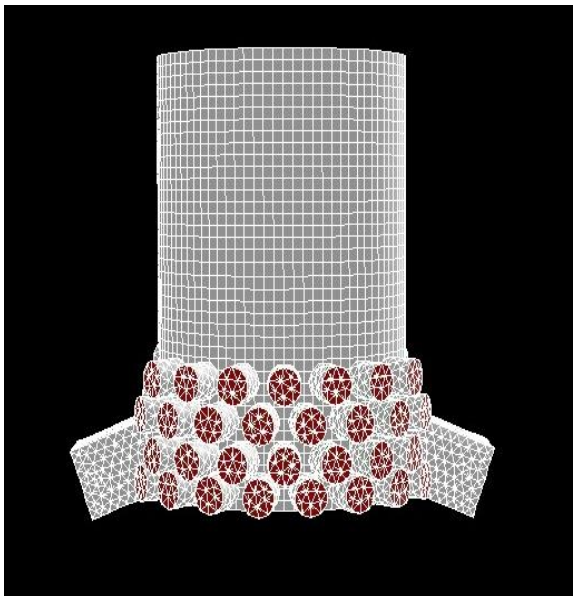

Fig. 3. 3D cylinder geometry with T-GRID type of mesh.

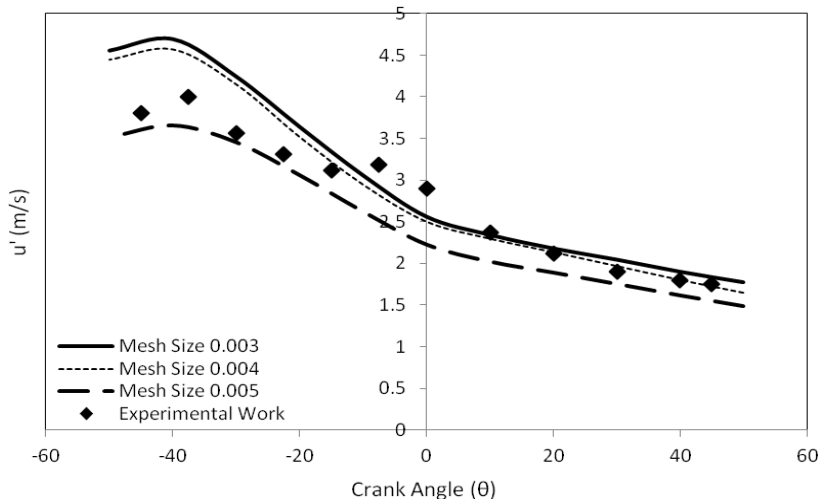

Fig. 4. Variation of RMS turbulent velocity (u') with crank angle (θ) at central point in the mid plan of the clearance volume using three different mesh size.

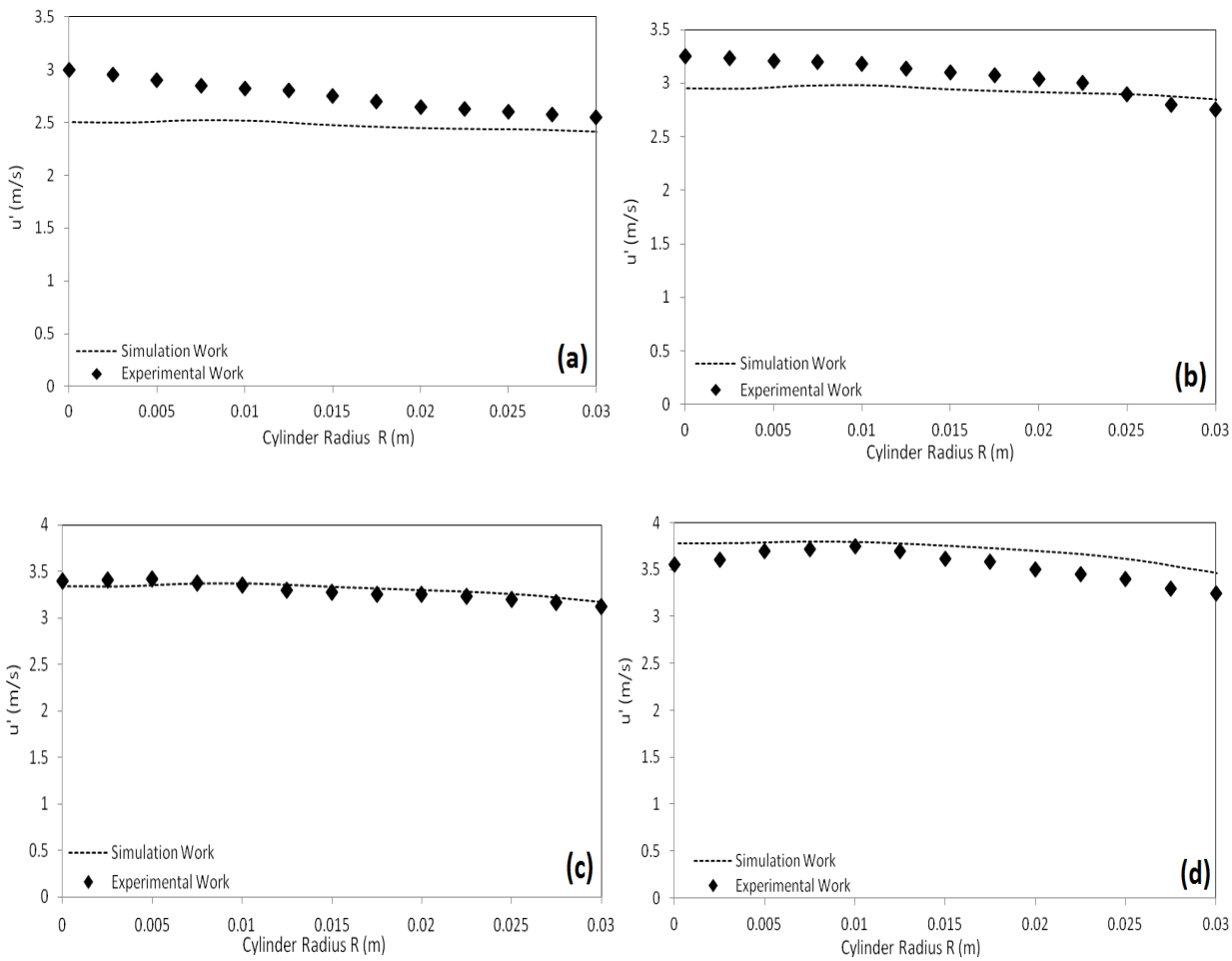

Fig. 5. RMS turbulent velocity for experimental and computational study along y-axis at (a) θ=0°, (b) θ= 10°, (c) θ= 17° and (d) θ= 24° BTDC.

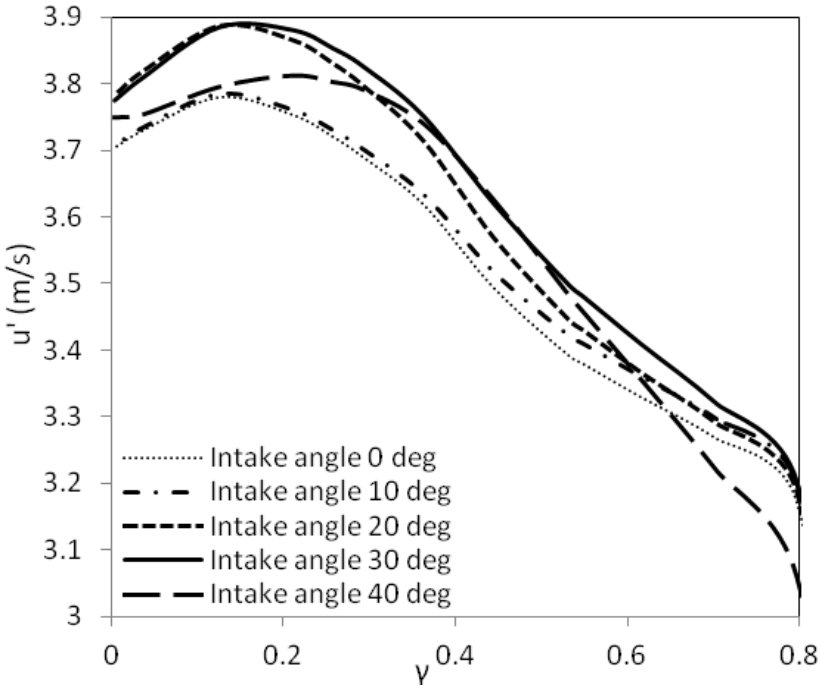

Fig. 6. RMS turbulent velocity along y-axis at θ = 24° BTDC and different α.

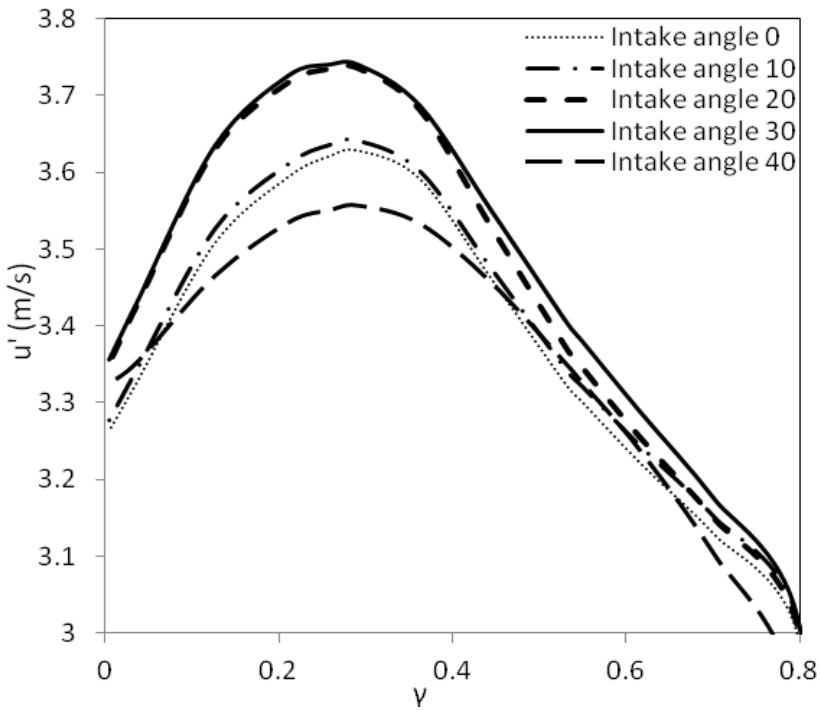

Fig. 7. RMS turbulent velocity along y-axis at θ = 17° BTDC and different α.

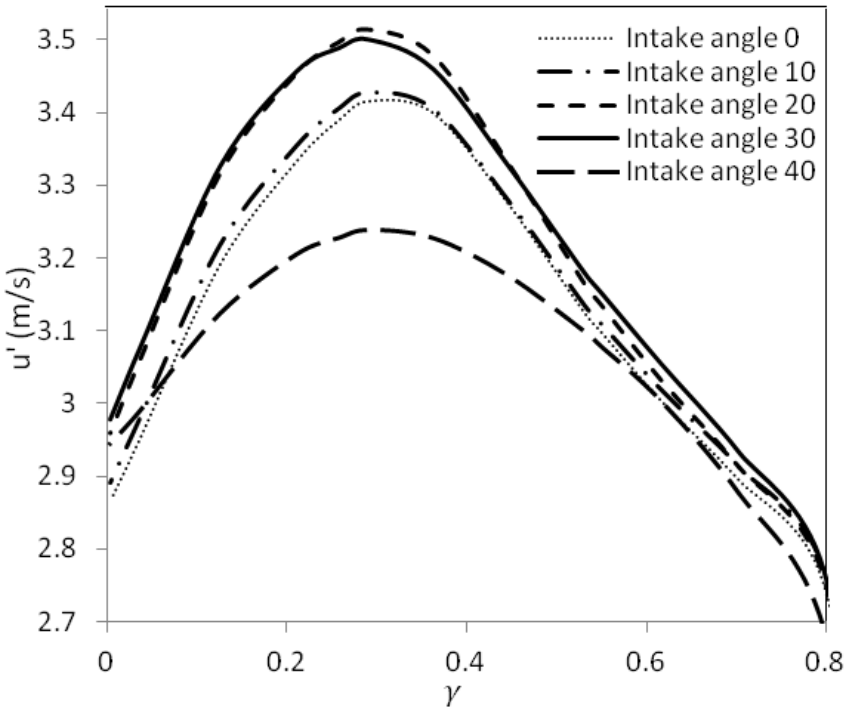

Fig. 8. RMS turbulent velocity along y-axis at θ = 10° BTDC and different α.

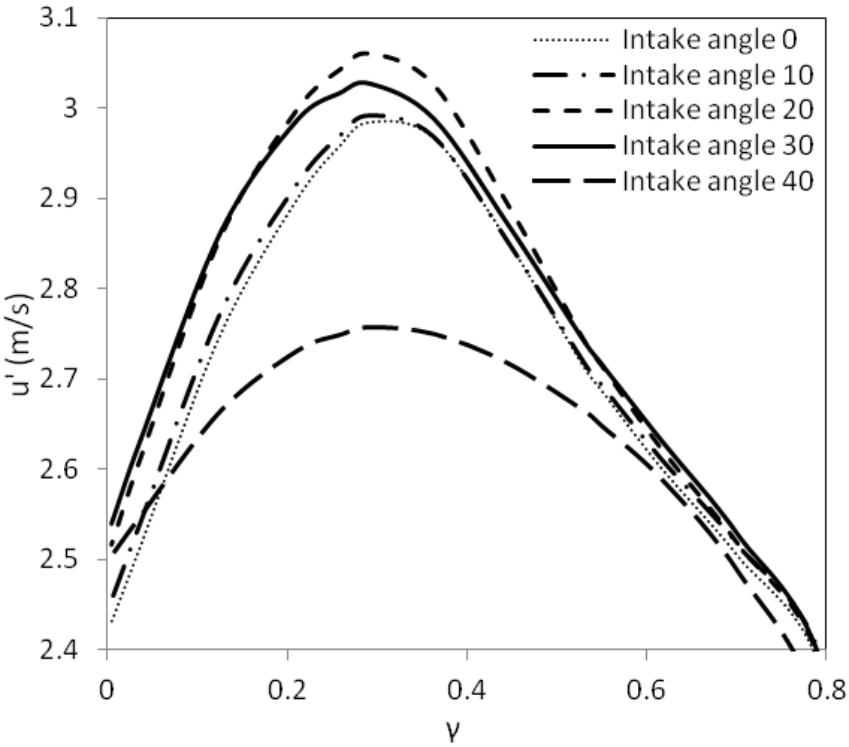

Fig. 9. RMS turbulent velocity along y-axis at θ = 0° BTDC and different α

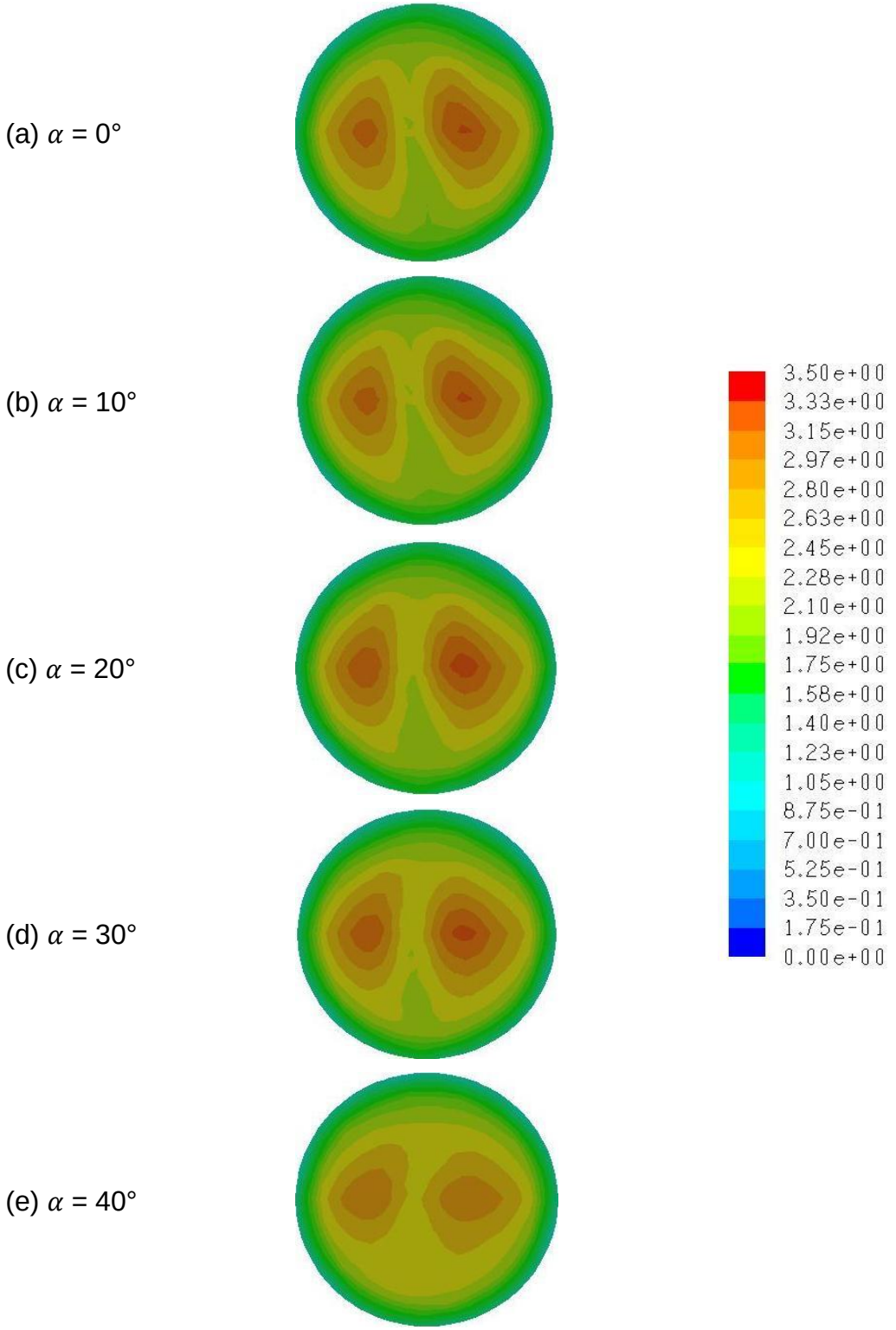

Fig. 10. u' counters at θ = 0° at TDC at different α